ACS OMEGA

http://pubs.acs.org/journal/acsodf

Article

Outer Membrane Vesicles Secreted by *Helicobacter pylori* Transmitting Gastric Pathogenic Virulence Factors

Sisi Wei,[#] Xiaoya Li,[#] Jingjing Wang, Yaojie Wang, Cong Zhang, Suli Dai, Xian Wang, Xiaoqing Deng, Lianmei Zhao,[*] and Baoen Shan[*]

Cite This: *ACS Omega* 2022, 7, 240−258

Read Online

ACCESS | Metrics & More | Article Recommendations | Supporting Information

ABSTRACT: *Helicobacter pylori* (*H. pylori*) is known to be a major pathogen causing gastric diseases through its direct localization in gastric epithelium cells. *H. pylori* releases outer membrane vesicles (OMVs) throughout the growth process. The content, function, and mechanism of *H. pylori* OMVs in gastric epithelial cells remain unclear. In this study, we extracted and characterized *H. pylori* OMVs of two strains (standard strain NCTC11637 and clinical strain Hp-400) and analyzed the specific content by proteomic technology. We identified more than 400 proteins in *H. pylori* OMVs. In addition, we investigated the impact of *H. pylori* OMVs on cellular functions by detecting proteomic changes in GES1 cells. GES1 cells cocultured with increasing concentrations of *H. pylori* OMVs were subjected to quantitative proteomic analyses using label-free methods for relative quantitation. The results showed that a total of 4261 proteins were verified, 153 of which were significantly altered in abundance when cocultured with NCTC11637 OMVs, and a total of 4234 proteins in Hp-400 OMVs, 390 of which were significantly altered. Gene ontology analysis and Kyoto encyclopedia of genes and genomes pathway mapping identified significantly altered inflammatory and cancer signaling pathways, including metabolic pathways and the PI3K-Akt signaling pathway. Furthermore, we explored the proteomic changes in GES1 cells induced by *H. pylori*. Bioinformatics analysis showed that changes in multiple pathways coincided with OMV-mediated proteomic changes. Based on these results, *H. pylori* induced pathogenicity in epithelial cells at least partially by secreting OMVs that mediated dramatic and specific proteomic changes in host cells. Data are available via ProteomeXchange with identifiers PXD025216, PXD025259, and PXD025281.

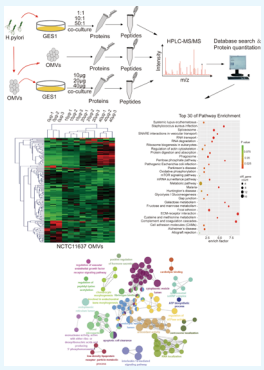

INTRODUCTION

Helicobacter pylori (*H. pylori*) is a spiral, microaerophilic, and Gram-negative bacterium that primarily colonizes the human stomach.[1] *H. pylori* persists in the human stomach lifelong and is predicted to have infected approximately half of the global population to cause multiple diseases, such as chronic gastritis, peptic ulcer, gastric mucosa-associated lymphoid tissue (MALT) lymphoma, and gastric cancer. *H. pylori* was also identified as a type I carcinogen by the WHO (World Health Organization) and contributes to a higher occurrence of gastric carcinoma.

Outer membrane vesicles (OMVs) are nanosized particles derived from the outer membrane of Gram-negative bacteria and play central roles in initiating and regulating pathogenesis in the host. OMVs generally have a diameter of 20−250 nm and are secreted under all environmental conditions and during all growth phases.[2,3] Originally considered as artifacts of the cell wall, OMVs are now accepted as a general secretion system.[4] OMVs carry a large amount of cargo from their parent bacterium, including virulence factors and toxins, such as outer membrane proteins, adhesins, invasions, proteases, and lipopolysaccharide (LPS),[5,6] illustrating that OMV secretion is an additional virulence mechanism of pathogens. The cargo may either be located in the vesicle lumen or integrated into the vesicle membrane.[7,8] Compared to other secretion systems, OMVs protect their contents from the external environment and transport their cargo over a long distance.[3,9]

Similar to other Gram-negative bacteria, *H. pylori* spontaneously secretes OMVs that play important roles in the pathogen−host interaction mechanism.[10] Several studies showed that the secreted *H. pylori* OMVs are internalized by gastric epithelial cells.[11−13] After internalization, OMVs regulate gastric epithelial cell proliferation, facilitate the secretion of inflammatory factors, and induce apoptosis.[12,14] In addition, *H. pylori* OMVs cause genomic instability in epithelial cells, as assessed using the cytokinesis-block micronuclei assay.[15] Furthermore, *H. pylori* OMVs induce human eosinophil degranulation.[16] Based on these results, we speculated that OMVs derived from *H. pylori* contributed to the *H. pylori*-induced pathogenic effects on the stomach.

Received: August 20, 2021
Accepted: December 3, 2021
Published: December 28, 2021

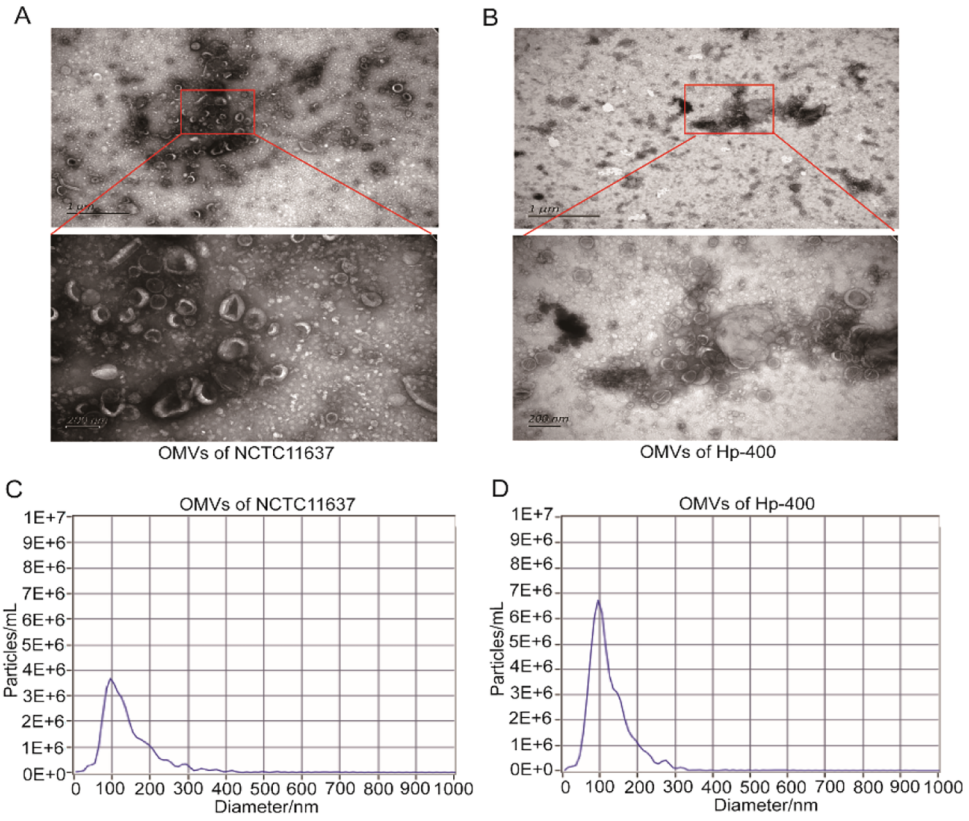

Figure 1. Purification and characterization of the *H. pylori* OMVs. (A) Representative TEM images of OMVs secreted by NCTC11637. (B) Representative TEM images of OMVs secreted by Hp-400. (C) NTA analysis of the size distributions and numbers of OMVs derived from NCTC11637. (D) NTA analysis of the size distributions and numbers of OMVs derived from Hp-400.

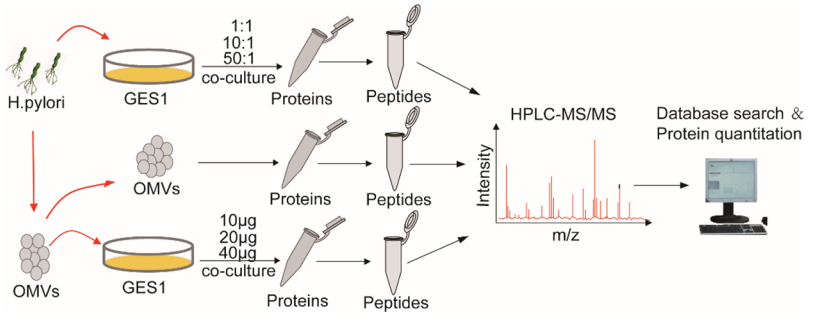

Figure 2. Schematic experimental workflow: First, the contents of purified OMVs were examined using HPLC-MS/MS. Then, GES1 cells cocultured with gradually increasing concentrations of OMVs and *H. pylori* were subjected to quantitative proteomic analysis. Finally, bioinformatics analysis was performed on the above data, on which basis, the exact pathways and proteins that changed in the infected GES1 cell proteome were characterized. The MS analysis of each sample was performed in triplicate, and data analysis was performed with the software PD2.2.

In this study, we purified and identified proteins in *H. pylori*-derived OMVs. We detected the protein contents of OMVs, including cagA, vacA, ureB, outer membrane proteins, and other virulence factors. We also found that *H. pylori* OMVs promoted the secretion of inflammatory cytokines, consistent with their parental bacteria. Furthermore, we identified proteomic changes in GES1 cells in response to OMVs or their parental bacteria. The bioinformatics analysis showed that multiple pathways overlapped, suggesting that OMVs contain most of the contents from their parental bacteria. Therefore, we highlight that *H. pylori* secretes and delivers gastric pathogenic virulence factors mostly via outer membrane vesicles.

RESULTS

Purification and Characterization of the *H. pylori* OMVs. *H. pylori* continuously secretes OMVs into the extracellular environment during growth. We collected a conditioned medium from NCTC11637 or Hp-400 and isolated OMVs after culturing for 72 h. Then, the *H. pylori* OMVs were characterized using nanoparticle tracking analysis (NTA) and transmission electron microscopy (TEM). TEM images revealed that the vesicles showed a spherical, bilayered morphology and a typical cup-shaped structure (Figure 1A,B). Additionally, NTA results showed that the size distribution of the OMVs ranged from 50 to 250 nm in diameter (Figure 1C,D), which is the typical size of OMVs produced by Gram-

https://doi.org/10.1021/acsomega.1c04549
ACS Omega 2022, 7, 240−258

Table 1. Protein Contents in NCTC11637 OMVs

number	accession	gene symbol	number	accession	gene symbol
1	P42383	groL	2	P56003	tuf
3	P69996	ureB	4	P0A0S1	flaA
5	P77872	katA	6	O26107	HP_1588
7	P56002	fusA	8	P55980	cagA
9	O25905	HP_1350	10	P55994	dnaK
11	P55987	atpA	12	P56418	acnB
13	O25242	dnaN	14	P56063	icd
15	P56112	HP_0175	16	P56185	rnj
17	P55975	tsf	18	P94845	glnA
19	P55988	atpD	20	P55969	hpaA
21	O25806	rpoBC	22	O25743	Ggt
23	O25294	pepA	24	O25017	HP_0231
25	P56116	htpG	26	P55981	vacA
27	O25284	HP_0558	28	P21762	ahpC
29	P52093	ftnA	30	P14916	ureA
31	P71404	clpB	32	O25011	msrAB
33	P56149	aspA	34	P0A0V0	lpp20
35	O25556	Omp19	36	P56088	guaB
37	P56008	rpsA	38	G2J5T2	hp1018/19
39	O25286	FabG	40	P50610	flgE
41	O25948	Ald	42	Q07911	flaB
43	O25750	Omp18	44	O06913	frdA
45	O25325	hemE	46	O25318	HP_0596
47	P43313	dps	48	O25751	tolB
49	O25349	HydB	50	O25739	HP_1111
51	P56420	tig	52	O26102	pdxJ
53	O25883	fumC	54	O25786	GlnH
55	O25656	PqqE	56	O25997	HP_1461
57	P56030	rplB	58	P56036	rplJ
59	O25749	HP_1124	60	O25546	HP_0879
61	O25321	HylB	62	O25371	YmxG
63	O24854	ribH	64	P56126	lysS
65	O24897	PutA	66	O25570	Omp20
67	O25015	Omp6	68	O24993	plsX
69	P56070	ppsA	70	O25326	HP_0605
71	O25135	HP_0371	72	O25216	PepF
73	O06914	frdB	74	O25736	HP_1108
75	P56001	rpoA	76	O25668	CbpA
77	A0A0M3KL20	C694_06140	78	O26082	CeuE
79	P56033	rplE	80	O25311	HP_0589
81	P56062	gltA	82	O24923	HP_0097
83	O24944	HP_0130	84	O25225	typA
85	O25534	pgbB	86	O25254	hslU
87	O25995	HP_1457	88	P96786	fliD
89	O26084	HP_1564	90	O25993	HP_1454
91	O25158	HP_0397	92	P56114	gatA
93	P56109	fba	94	O25825	HP_1227
95	O25856	NQO3	96	O34523	Omp29
97	O25927	lpxA	98	O25134	HP_0370
99	O25399	HP_0690	100	P56029	rplA
101	O25738	HP_1110	102	O25414	HP_0710
103	O25423	HP_0721	104	O25347	HP_0630
105	O25715	HP_1083	106	P56456	ileS
107	P56145	pheT	108	P56031	rplC
109	O24914	HP_0087	110	O25732	Cad
111	O25116	pyrG	112	O25383	HP_0672
113	O25787	HP_1173	114	O25166	HP_0410
115	O25052	AddB	116	O25465	HP_0773
117	O25008	iscS	118	O25067	amiE
119	P56060	kdsA	120	O25658	HdhA
121	O25936	fbp	122	P55982	nrdA

https://doi.org/10.1021/acsomega.1c04549
ACS Omega 2022, 7, 240−258

Table 1. continued

number	accession	gene symbol	number	accession	gene symbol
123	O25089	HP_0322	124	P66928	trxA
125	P56047	rplV	126	O24990	fabI
127	P0A0R3	groS	128	O26104	FlgG
129	O25560	hypB	130	O25571	Omp21
131	O25873	HP_1286	132	P56078	rplY
133	O25608	rdxA	134	O25410	Omp15
135	O24913	mqo	136	O25312	HP_0590
137	P56004	efp	138	O25925	mreB
139	P56431	trxB	140	O25327	MtrC
141	P25177	glmM	142	O25147	HP_0385
143	P56111	edd	144	P56146	pheS
145	O25731	glk	146	O25820	Dld
147	O25372	gatB	148	P56034	rplF
149	P42445	recA	150	P56460	metK
151	P56071	thrS	152	O25088	tatA
153	P56154	pgk	154	P56458	serS
155	O24922	HP_0096	156	O25009	HP_0221
157	P56032	rplD	158	O24925	TlpA
159	O24911	TlpC	160	O26004	ilvE
161	O25373	HP_0659	162	O24870	Omp2
163	Q09066	ureG	164	O25776	fldA
165	O25720	TktA	166	O25079	HP_0309
167	O24924	thrC	168	P56082	atpG
169	O25503	speE	170	P55972	infB
171	P56457	leuS	172	O25313	HP_0591
173	O25034	Omp7	174	P56155	pyrF
175	P64655	HP_0135	176	P55995	lon
177	O25872	HP_1285	178	O26075	yajC
179	P66609	rpsG	180	P94851	HP_1488
181	O25744	HAP1	182	O25140	DsbC
183	O24947	HP_0134	184	Q48248	cdh
185	O25151	tpx	186	O25779	TrxB
187	O25046	HP_0267	188	P71408	ftsH
189	P55834	rplL	190	O25018	HP_0232
191	P56046	rplU	192	O25341	AspB
193	P66328	rpsJ	194	P56035	rplI
195	O25597	dadA	196	O25369	bamA
197	O25389	HP_0678	198	P96551	gltX1
199	O25684	HP_1043	200	O24886	fcl
201	O25671	fur	202	P66572	rpsE
203	P56069	metB	204	O25607	HP_0953
205	O25029	rhpA	206	O25756	AtpH
207	O25530	RfaD	208	P48285	eno
209	P66052	rplK	210	O25625	HP_0973
211	O25728	hcpC	212	P56089	glyA
213	O25729	HP_1099	214	O24976	HP_0170
215	P56007	scoB	216	O25249	pgbA
217	O25762	HP_1143	218	P56106	pyrH
219	O25998	HP_1462	220	P56459	aspS
221	O25068	Fla	222	O24951	HP_0139
223	P66637	rpsI	224	O25036	Omp8
225	P56191	ddl	226	P56052	rpmC
227	O25087	hugZ	228	P48370	gyrA
229	O25080	pgdA	230	O25276	Cag22
231	O25157	HP_0396	232	O25773	proC
233	O25996	HP_1458	234	O25424	ansA
235	P56020	rpsM	236	O25283	accA
237	O25342	ispG	238	O25442	HP_0746
239	P56038	rplM	240	P56009	rpsB
241	O25771	Omp25	242	P56011	rpsD
243	O25001	hcpA	244	P56041	rplP

https://doi.org/10.1021/acsomega.1c04549
ACS Omega 2022, 7, 240−258

Table 1. continued

number	accession	gene symbol	number	accession	gene symbol
245	O24996	HP_0204	246	P66449	rpsQ
247	O25164	HP_0408	248	O25681	HP_1037
249	Q48255	aroQ	250	P56018	rpsK
251	P0A0X4	rpsL	252	O25791	Omp27
253	P56417	tyrS	254	O25999	HP_1463
255	P56010	rpsC	256	O25250	GlcD
257	O25572	HP_0914	258	P56006	scoA
259	O25176	HP_0422	260	O24999	mrp
261	P56156	clpP	262	O25360	gltX2
263	O26037	HP_1507	264	O25413	HP_0709
265	O25229	HP_0485	266	O25781	pgi
267	O25564	HP_0906	268	P56039	rplN
269	P56084	atpC	270	O25673	HP_1029
271	O24949	HP_0137	272	O25452	HP_0757
273	O25553	HP_0893	274	O24865	HP_0020
275	O26035	RibG	276	O25949	HP_1399
277	O25255	HP_0518	278	O26083	CeuE
279	O25213	HP_0466	280	O25253	hslV
281	O25006	HP_0218	282	P55992	gyrB
283	O24950	HP_0138	284	O25280	HP_0554
285	P56141	trpA	286	P56110	zwf
287	O25076	HP_0305	288	O25926	clpX
289	O25930	bamD	290	P56045	rplT
291	P56097	ftsZ	292	O25899	tonB
293	P56128	argS	294	O25489	HP_0809
295	O25664	ispDF	296	O25234	HP_0492
297	O25511	pseB	298	O25737	HP_1109
299	P64653	HP_0122	300	O25516	thiM
301	O25990	HP_1451	302	O25801	asd
303	O25310	HP_0588	304	O24934	HP_0112
305	O25030	HP_0248	306	O24943	HP_0129
307	O24941	Omp4	308	P56086	atpF
309	P56455	hisS	310	P55970	grpE
311	O25566	HP_0908	312	P56044	rplS
313	O25524	YheS	314	O25257	Cag1
315	O25982	ppiA	316	O25470	HP_0781
317	O25992	HP_1453	318	O25931	TyrA
319	P66185	rpmE	320	P56162	pyrE
321	O25853	nuoD	322	P56067	cysM
323	O24884	HP_0043	324	O25510	OmpP1
325	O25421	HP_0719	326	P56075	ndk
327	P55976	nusG	328	O24991	lpxD
329	P56396	trpS	330	O25019	HP_0233
331	O25529	hldE	332	O25614	gpsA
333	P43312	sodB	334	O26067	HP_1542
335	P56021	rpsZ	336	O25565	FlgD
337	O25858	nuoI	338	O25759	Soj
339	O25584	surE	340	P66119	rplW
341	P56000	valS	342	P55971	gapA
343	O25362	Slt	344	P55985	truD
345	O25758	parB	346	O25782	HP_1167
347	O25343	dapD	348	O25032	OppD
349	O25956	bioB	350	O26094	RibC
351	O25686	acsA	352	O25748	slyD
353	O25953	HsdM	354	P66621	rpsH
355	Q59465	cadA	356	O25277	Cag24
357	O25171	Cfa	358	P56124	proS
359	P56040	rplO	360	P55979	bcp
361	P56195	deoB	362	O25913	HP_1359
363	O25521	HsdM	364	O25132	HP_0368
365	O25757	AtpF′	366	O25896	HP_1338

https://doi.org/10.1021/acsomega.1c04549
ACS Omega 2022, 7, 240−258

Table 1. continued

number	accession	gene symbol	number	accession	gene symbol
367	O25525	guaC	368	O25121	dxs
369	O25549	ruvA	370	P56104	adk
371	O25293	ychF	372	O25595	alr
373	P56737	trpD	374	O26103	pdxA
375	P56137	purA	376	P56452	alaS
377	P94842	ybgC	378	O24885	gmd
379	O24864	CheV	380	P56184	prs
381	O25475	secA	382	O25477	HP_0788
383	O24973	OmpR	384	O26096	metN
385	P56157	dnaE	386	O24890	HP_0049
387	O26064	HP_1539	388	O25533	coaX
389	P56115	hemL	390	O25577	carB
391	P56176	nnr	392	O25335	HP_0614
393	P56153	ppa	394	O25469	HP_0780
395	O25624	HP_0971	396	O25376	hemN
397	O25929	fliW2	398	O25281	HP_0555
399	O25233	HP_0490	400	O25398	HP_0689
401	O25435	Gpt	402	O24994	fabH
403	O25136	dcd	404	P56022	rpsO
405	O26074	secD	406	P56074	hemB
407	O25382	Omp14	408	O25991	mnmE
409	O25945	Omp30	410	P55990	gdhA
411	P56028	rpsU	412	O25430	HP_0730
413	O25696	HP_1056	414	O25122	lepA
415	O25390	WbpB	416	P56127	metG
417	O25348	HydA	418	P56142	trpB
419	O25902	Gap	420	P56122	aroC
421	O25849	cobB	422	O24956	FixO
423	O25308	HP_0586	424	O25484	ribB
425	O25594	YckK	426	O25817	purD
427	O25500	Lex2B	428	P56131	miaB
429	O25055	GppA	430	O25195	HP_0447
431	O25912	HP_1358	432	O25142	HP_0379
433	O25363	HP_0646	434	O25082	HP_0312
435	O25509	HP_0838	436	O25278	Cag25

negative bacteria. Taken together, we successfully purified *H. pylori* OMVs.

Subsequently, in order to detect the proteomic changes in GES1 cells cocultured with gradually increasing concentrations of OMVs and *H. pylori* as well as to reveal the influence of OMVs and *H. pylori* on host gastric epithelial cells, an experimental scheme focused on the HPLC-MS/MS method was adopted and its workflow is shown in Figure 2.

Identification of the Protein Contents of *H. pylori* OMVs. Next, we determined the protein contents of *H. pylori* OMVs to evaluate the mechanisms by which these components confer their immunomodulatory and cytotoxic activities to host cells, as these disease-associated activities are also transferred by the bacterium from which the vesicles are derived. We detected the protein contents of OMVs using HPLC-MS/MS analysis, and 436 proteins were found in NCTC11637 OMVs (Table 1) and 372 proteins in Hp-400 OMVs (Table 2). Although a significant overlap in the proteins identified between NCTC11637 and Hp-400 was observed, not all proteins appeared to be shared, suggesting that these two *H. pylori* strains have different genotypes (Figure 3A). The proteomic analysis illustrated the enrichment of membrane proteins, adhesins, porins, and several proteins known to regulate cell proliferation, cytokine secretion, and other host cellular processes in *H. pylori* OMVs. In addition, the OMVs contained the previously documented toxins cagA, vacA, and several OMV components possessing immunological activity, including urease, HpaA, OMP18, peptidyl-prolyl-*cis*-*trans*-isomerase, and gamma-glutamyl transpeptidase (Tables 1 and 2). Furthermore, the GO analysis revealed similar cellular components for the OMV contents in the two strains, mainly including the cytoplasmic part, such as the cytoplasm and cytomembrane (Figure 3B,C). Taken together, the *H. pylori* OMVs are equipped with the molecules required to interact with host cells in a manner similar to the intact pathogen.

***H. pylori* OMVs Promoted the Secretion of Inflammatory Factors of GES1 Cells.** *H. pylori* colonizes the gastric mucosa and causes acute and chronic gastritis accompanied by a chronic pro-inflammatory environment, and thus the inflammatory response is the main characteristic of *H. pylori* infection. As shown above, OMVs contain a variety of virulence factors; therefore, we hypothesized that OMVs induce inflammation similar to the bacterium from which they are derived. Inflammatory factors were detected in the cultured supernatant of GES1 cells cocultured with OMVs (40 μg) or *H. pylori* (50:1). The levels of secreted IL-5, IL-6, IFN-γ, IL-8, IL-12P70, and TNF-α were significantly increased when cells were cocultured with either OMVs or *H. pylori* (Figure 4A). In particular, IL-6,

https://doi.org/10.1021/acsomega.1c04549
ACS Omega 2022, 7, 240−258

Table 2. Protein Contents in Hp-400 OMVs

number	accession	gene symbol	number	accession	gene symbol
1	P42383	groL	2	P56003	tuf
3	P69996	ureB	4	P77872	katA
5	O25806	rpoBC	6	G2J5T2	hp1018/19
7	O26107	HP_1588	8	O24870	Omp2
9	P55987	atpA	10	O25743	HP_1118
11	P56418	acnB	12	P55975	tsf
13	P56063	icd	14	O25011	msrAB
15	P0A0V0	lpp20	16	P71404	clpB
17	P55969	hpaA	18	P55994	dnaK
19	O25905	HP_1350	20	O25286	HP_0561
21	O25751	tolB	22	P94845	glnA
23	O25242	dnaN	24	P55988	atpD
25	O25791	Omp27	26	A0A0M3KL20	C694_06140
27	P56002	fusA	28	O25017	HP_0231
29	O25311	HP_0589	30	O25825	HP_1227
31	O25321	HP_0599	32	O25294	pepA
33	O26083	HP_1562	34	O25423	HP_0721
35	P14916	ureA	36	O06913	frdA
37	O25732	HP_1104	38	O25284	HP_0558
39	O25052	AddB	40	P56008	rpsA
41	O25015	Omp6	42	O25786	GlnH
43	O24925	TlpA	44	P56112	HP_0175
45	O25749	HP_1124	46	O26084	HP_1564
47	P56456	ileS	48	P50610	flgE
49	O25840	Omp28	50	P21762	ahpC
51	P55981	vacA	52	P52093	ftnA
53	P56036	rplJ	54	O25993	HP_1454
55	P56149	aspA	56	O25312	HP_0590
57	O25883	fumC	58	O25216	PepF
59	O25147	HP_0385	60	O25656	PqqE
61	O25997	HP_1461	62	P56062	gltA
63	O25738	HP_1110	64	O25414	HP_0710
65	P56185	rnj	66	O25736	HP_1108
67	P56145	pheT	68	O26082	CeuE
69	P56155	pyrF	70	O24968	pyrF
71	O26102	pdxJ	72	O25995	HP_1457
73	O25927	lpxA	74	O25750	Omp18
75	O24944	HP_0130	76	O25157	HP_0396
77	O24923	HP_0097	78	O25872	HP_1285
79	O25046	HP_0267	80	P56116	htpG
81	O24922	HP_0096	82	O25729	Eda
83	O25992	HP_1453	84	O25158	HP_0397
85	O25597	dadA	86	O24993	plsX
87	O25055	GppA	88	O25510	OmpP1
89	O25229	HP_0485	90	P55982	nrdA
91	O25556	Omp19	92	P66928	trxA
93	P55993	rpoD	94	O25402	HyuA
95	O25135	HP_0371	96	O25349	HydB
97	O25728	hcpC	98	P0A0R3	groS
99	P43313	dps	100	P56070	ppsA
101	O25757	AtpF′	102	O26042	FrpB
103	O25739	HP_1111	104	O25326	HP_0605
105	O25371	YmxG	106	O25225	typA
107	O06914	frdB	108	P56030	rplB
109	O25088	tatA	110	P56060	kdsA
111	P56047	rplV	112	P55980	cagA
113	P56111	edd	114	O25313	HP_0591
115	O25045	pyrC′	116	P56420	tig
117	O25776	fldA	118	O25257	Cag1
119	P56088	guaB	120	O25771	Omp25
121	O25936	fbp	122	O25176	HP_0422

https://doi.org/10.1021/acsomega.1c04549
ACS Omega 2022, 7, 240−258

Table 2. continued

number	accession	gene symbol	number	accession	gene symbol
123	P56007	scoB	124	O25948	Ald
125	P56078	rplY	126	P56431	trxB
127	O25570	Omp20	128	O25756	AtpH
129	O25399	FadA	130	P25177	glmM
131	O25715	HP_1083	132	O25787	HP_1173
133	P56034	rplF	134	O25658	HdhA
135	O25607	HP_0953	136	O25369	bamA
137	P56110	zwf	138	O25318	HP_0596
139	O25562	HP_0902	140	O25076	HP_0305
141	O26071	HP_1546	142	O25625	HP_0973
143	O24996	HP_0204	144	P56001	rpoA
145	O25410	Omp15	146	O25325	hemE
147	O25781	pgi	148	O25153	CheA
149	O26067	HP_1542	150	O24913	mqo
151	O24947	HP_0134	152	O25403	HP_0696
153	P56154	pgk	154	O25465	HP_0773
155	P42445	recA	156	O24914	HP_0087
157	O24911	TlpC	158	O24897	PutA
159	O25327	MtrC	160	O25534	pgbB
161	P56146	pheS	162	O25442	HP_0746
163	O25773	proC	164	O25742	HP_1117
165	O25503	speE	166	O24881	HP_0040
167	P56458	serS	168	O25372	gatB
169	O24950	HP_0138	170	O25373	HP_0659
171	O25998	HP_1462	172	P56114	gatA
173	O25546	HP_0879	174	O25668	CbpA
175	P56067	cysM	176	O25469	HP_0780
177	O25249	pgbA	178	O25069	DppA
179	O25873	HP_1286	180	O25230	HP_0486
181	O24909	HP_0080	182	P56106	pyrH
183	O25470	HP_0781	184	P56046	rplU
185	P56126	lysS	186	O25458	ftsY
187	P56082	atpG	188	P56075	ndk
189	O25273	Cag19	190	P56006	scoA
191	O25140	DsbC	192	O25926	clpX
193	P56109	fba	194	P56460	metK
195	O25134	HP_0370	196	O25213	HP_0466
197	Q48248	cdh	198	P56127	metG
199	P64655	HP_0135	200	P56052	rpmC
201	O26091	rlpA	202	P56031	rplC
203	Q09066	ureG	204	O25018	HP_0232
205	O25902	Gap	206	P56457	leuS
207	O24929	TlpB	208	O25009	NifU
209	O25424	ansA	210	O26031	Omp32
211	O25564	HP_0906	212	P56104	adk
213	O25477	HP_0788	214	O25475	secA
215	P56035	rplI	216	O25474	lolA
217	O25165	guaA	218	O25283	accA
219	P56468	purB	220	O25574	FrpB
221	O24924	thrC	222	O25572	HP_0914
223	P56004	efp	224	P56032	rplD
225	O25452	HP_0757	226	P56455	hisS
227	O25508	HP_0837	228	P56137	purA
229	O25036	Omp8	230	O25925	mreB
231	O25594	YckK	232	P56459	aspS
233	O24949	HP_0137	234	O25999	HP_1463
235	P56018	rpsK	236	O25820	Dld
237	P56029	rplA	238	O25255	HP_0518
239	O24863	HP_0018	240	O25087	hugZ
241	O26037	HP_1507	242	P56084	atpC
243	O24930	CpdB	244	P56020	rpsM

https://doi.org/10.1021/acsomega.1c04549
ACS Omega 2022, 7, 240−258

Table 2. continued

number	accession	gene symbol	number	accession	gene symbol
245	O25368	mqnE	246	P55970	grpE
247	O25218	Omp11	248	P64653	HP_0122
249	O25234	HP_0492	250	O25383	HP_0672
251	O25762	HP_1143	252	P66637	HP_1143
253	O26039	plsY	254	O24864	CheV
255	O26052	HP_1524	256	O25073	DppF
257	O24999	mrp	258	O25684	HP_1043
259	P56041	rplP	260	O25288	HP_0564
261	P56039	rplN	262	O25930	BamD
263	O24951	HP_0139	264	O25089	HP_0322
265	O25426	HP_0726	266	O25116	pyrG
267	O25256	HP_0519	268	P94844	dapB
269	P66052	rplK	270	O25573	FrpB
271	O25856	NQO3	272	O25713	HP_1081
273	O25276	Cag22	274	O25362	Slt
275	O25355	Omp13	276	O25090	Nuc
277	O25472	HP_0783	278	P56089	glyA
279	P64649	HP_0031	280	P56033	rplE
281	O24854	ribH	282	O24941	Omp4
283	O34523	Omp29	284	O25770	murG
285	O25595	alr	286	O25336	ligA
287	O25489	HP_0809	288	P56044	rplS
289	O26004	ilvE	290	P55971	gapA
291	P56069	metB	292	O25289	HP_0565
293	P56086	atpF	294	P48285	eno
295	O25152	CheW	296	O24946	SdaC
297	P56197	aroA	298	O25297	HP_0573
299	O25397	HP_0688	300	O25990	HP_1451
301	O24865	HP_0020	302	O25343	dapD
303	O87326	trl	304	O25507	HP_0836
305	O25171	Cfa	306	O25681	HP_1037
307	O24871	HP_0028	308	O25161	HP_0405
309	P94851	HP_1488	310	O25072	DppD
311	O25029	rhpA	312	O25571	Omp21
313	O25530	RfaD	314	O25696	HP_1056
315	O25671	fur	316	O25144	YJR117W
317	P55995	lon	318	O25079	HP_0309
319	O25560	hypB	320	O26096	metN
321	O25509	HP_0838	322	O25612	HP_0958
323	P66119	rplW	324	O25512	CoaBC
325	O25296	apt	326	O25032	OppD
327	P56061	panC	328	O25281	HP_0555
329	O25748	slyD	330	O25484	ribB
331	P66328	rpsJ	332	O25250	GlcD
333	O25337	CheV	334	O25584	surE
335	P56467	folD	336	O24886	fcl
337	O26075	yajC	338	P56072	sdaA
339	P56011	rpsD	340	O25772	Omp26
341	O24991	lpxD	342	O25166	HP_0410
343	O25039	xseA	344	P55972	infB
345	O25382	Omp14	346	O25348	HydA
347	P56191	ddl	348	P56153	ppa
349	O25413	HP_0709	350	O25714	MsbA
351	O25673	HP_1029	352	O25991	mnmE
353	P66572	rpsE	354	P55834	rplL
355	P56000	valS	356	P55992	gyrB
357	P56040	rplO	358	O25945	Omp30
359	O25535	HP_0864	360	O25008	iscS
361	P55976	nusG	362	P55986	HP_1459
363	O25347	Mda66	364	P56038	rplM
365	O25274	Cag20	366	O25151	tpx

https://doi.org/10.1021/acsomega.1c04549
ACS Omega 2022, 7, 240−258

Table 2. continued

number	accession	gene symbol	number	accession	gene symbol
367	O25852	HP_1262	368	P56022	rpsO
369	P56156	clpP	370	O25931	TyrA
371	O25614	gpsA	372	P56097	ftsZ

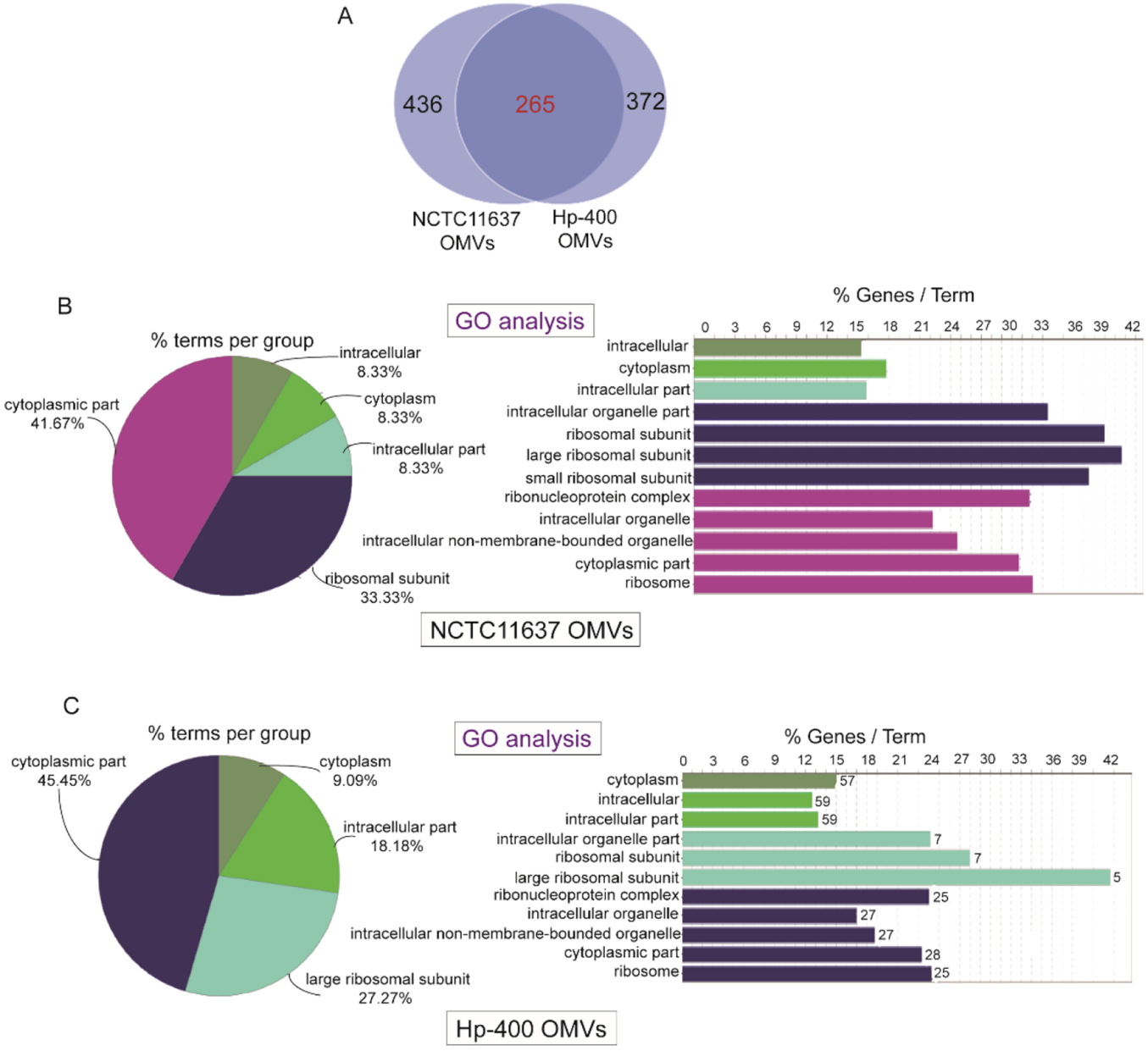

Figure 3. Identification of protein contents of *H. pylori* OMVs. (A) Proteins in NCTC11637 and Hp-400 detected by HPLC-MS/MS. (B) Cellular components of NCTC11637 OMV contents revealed by GO analysis. (C) Cellular components of Hp-400 OMV contents revealed by GO analysis.

IL-8, and TNF-α play an important role in the activation of neutrophils and lymphocytes and the induction of T cell activation, proliferation, and differentiation. The levels of other inflammatory factors, IL-2, IL-10, and IL-17, were also slightly increased (Figure 4B), although the difference was not significant. Additionally, we did not observe a difference in cytokine levels between *H. pylori*-treated cells and OMV-treated cells, suggesting that *H. pylori* induced an inflammatory response mainly through OMVs.

The Proteomic Changes in GES1 Cells Cocultured with NCTC11637 OMVs Were Consistent with Those of GES1 Cells Cocultured with the NCTC11637 Strain. GES1 cells were cocultured with increasing concentrations of OMVs (0, 10, 20, or 40 μg) or bacteria (control, 1:1, 10:1, or 50:1) and subjected to quantitative proteomic analyses using label-free methods for relative and absolute quantitation to further define the effects of NCTC11637 OMVs and the parental strain on gastric epithelial cells. A total of 4261 proteins were quantified in GES1 cells cocultured with OMVs, 79, 128, and 153 of which

https://doi.org/10.1021/acsomega.1c04549
ACS Omega 2022, 7, 240−258

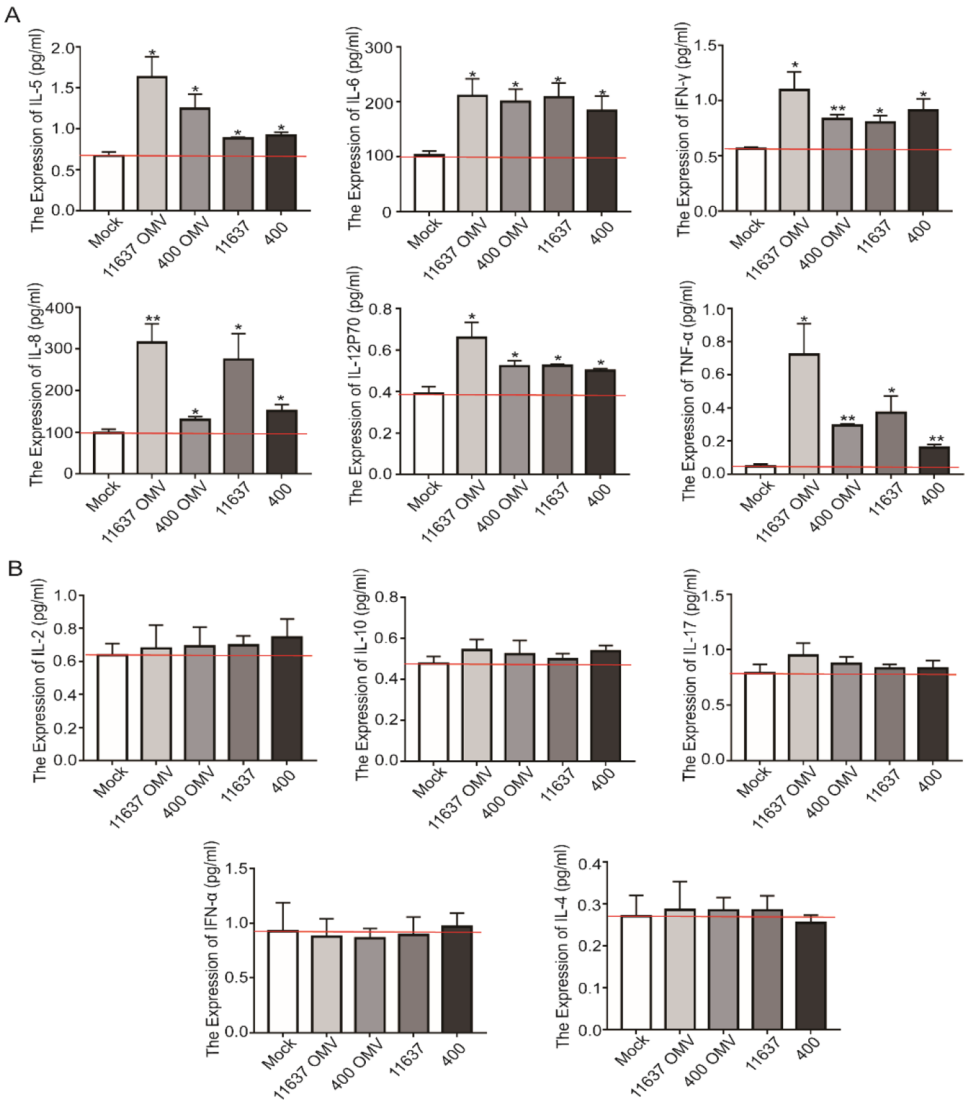

Figure 4. *H. pylori* and OMVs induced secretion of inflammatory factors. (A) Inflammatory factors, IL-5, IL-6, IFN-γ, IL-8, IL-12P70, and TNF-α, in the cultural supernatant were detected by flow cytometry. (B) Inflammatory factors, IL-2, IL-10, IL-17, IFN-α, and IL-4, the in cultural supernatant were detected by flow cytometry. *$p < 0.05$, **$p < 0.01$.

were markedly changed (|fold change| > 2) in abundance after treatment with 10, 20, and 40 μg of OMVs, respectively, compared to control samples (Figure 5A and Supporting information Table S1); we described the difference in the proteome of cells treated with OMVs (40 μg). KEGG and GO analyses were next used to find biologically relevant canonical signaling pathways that were significantly altered by OMVs. In the KEGG pathway analysis, RNA transport and degradation, oxidative phosphorylation, metabolism, tight junctions, cytoskeleton, and extracellular matrix signaling were significantly altered (Figure 5B). In the GO analysis, including biological processes, cellular components and molecular functions, IL-12 signaling pathways, VEGF receptor pathway, antioxidant activity, apoptosis, and other terms were dramatically altered (Figure 5C). These pathways are related to immune regulation and carcinogenesis.

Similarly, we identified 4360 proteins in GES1 cells cocultured with the NCTC11637 strain; 53, 165, and 367 proteins displayed significantly altered abundance (|fold change| > 2) after infection with the bacteria at multiplicities of infection (MOIs) of 1:1, 10:1, and 50:1, respectively, compared to uninfected samples (Figure 5D and Supporting information Table S2). Therefore, we analyzed the proteome of infected GES1 cells in the 50:1 group. The KEGG analysis showed significant changes in amino acid metabolism, p53 signaling pathway, ECM-receptor interaction, and epithelial cell signaling in response to the *H. pylori* infection (Figure 5E). The GO analysis revealed that T cell-mediated immunity, integrin binding, mitotic cell cycle, antioxidant activity, and chromosome organization were dramatically altered (Figure 5F) in response to NCTC11637 infection.

In addition, 35 proteins overlapped between the proteomes of GES1 cells infected with NCTC11637 and OMVs (Figure 5G). Furthermore, the top 10 hub genes were screened (Figure 5H). Taken together, these results revealed that NCTC11637 OMVs led to changes in the GES1 cell proteome and the altered pathways mapped to the donor bacteria.

The Proteomic Changes in GES1 Cells Cocultured with Hp-400 OMVs Were in Accordance with Those of GES1 Cells Cocultured with Hp-400. Another *H. pylori* strain, Hp-400, was used to detect proteomic changes in cells cocultured with OMVs or the *H. pylori* strain and to further confirm our

https://doi.org/10.1021/acsomega.1c04549
ACS Omega 2022, 7, 240−258

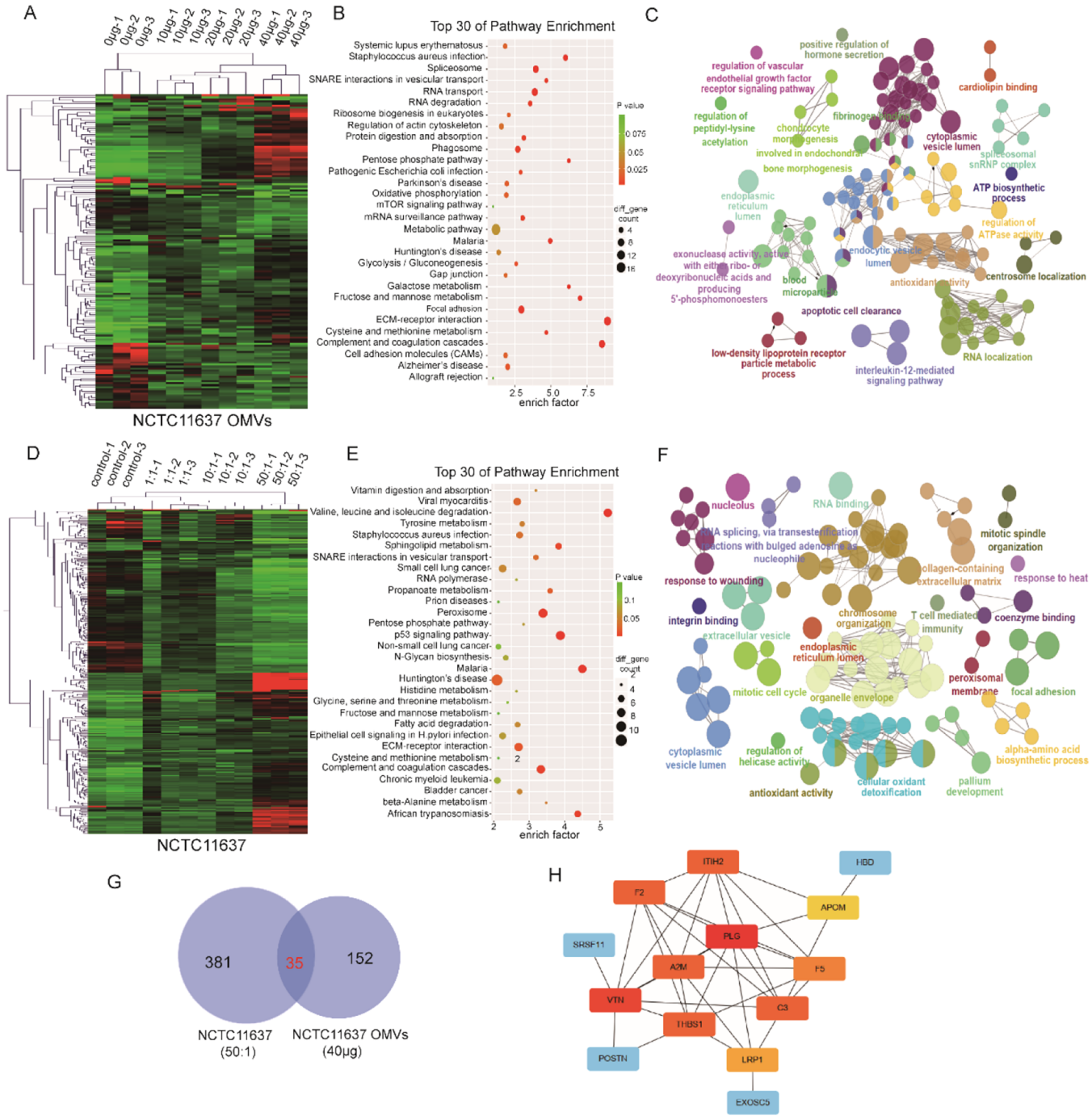

Figure 5. Proteomic changes of GES1 infected by NCTC11637 OMVs and bacteria. (A) Heat map showing differentially expressed proteins in different groups of GES1 cocultured with increasing NCTC11637 OMVs (0, 10, 20, and 40 μg/well). (B) KEGG analysis of differentially expressed proteins in GES1 control and GES1 cocultured with 40 μg of NCTC11637 OMVs. (C) GO analysis of differentially expressed proteins in GES1 control and GES1 cocultured with 40 μg of NCTC11637 OMVs. (D) Heat map showing differentially expressed proteins in different groups of GES1 cocultured with increasing NCTC11637 (0, 1:1, 10:1, and 50:1). (E) KEGG analysis of differentially expressed proteins in GES1 control and GES1 cocultured with 50:1 NCTC11637. (F) GO analysis of differentially expressed proteins in GES1 control and GES1 cocultured with 50:1 NCTC11637. (G) Venn diagram revealed the overlapped proteins between differentially expressed proteins in GES1 infected by NCTC11637 and OMVs. (H) Top 10 hub genes of the overlapped proteins in panel G.

hypothesis that OMVs play vital roles in *H. pylori*-treated GES1 cells. Hp-400 is a clinical strain isolated from northern China, where the incidence of gastric cancer is high. Consistent with our hypothesis, the quantitative proteomic analysis verified a total of 4234 proteins in GES1 cells cocultured with Hp-400 OMVs, 303, 236, and 390 of which exhibited significantly altered (|fold change| > 1.5) abundance following infection with 10, 20, and 40 μg of Hp-400 OMVs, respectively, compared to uninfected samples (Figure 6A and Supporting information Table S3). Consistent with the aforementioned findings, we described the GES1 proteomic change induced by OMVs (40 μg). The KEGG analysis revealed marked changes in several pathways, including amino acid metabolism, spliceosome, RNA process, and protein exporting (Figure 6B). The GO analysis showed significant

https://doi.org/10.1021/acsomega.1c04549
ACS Omega 2022, 7, 240−258

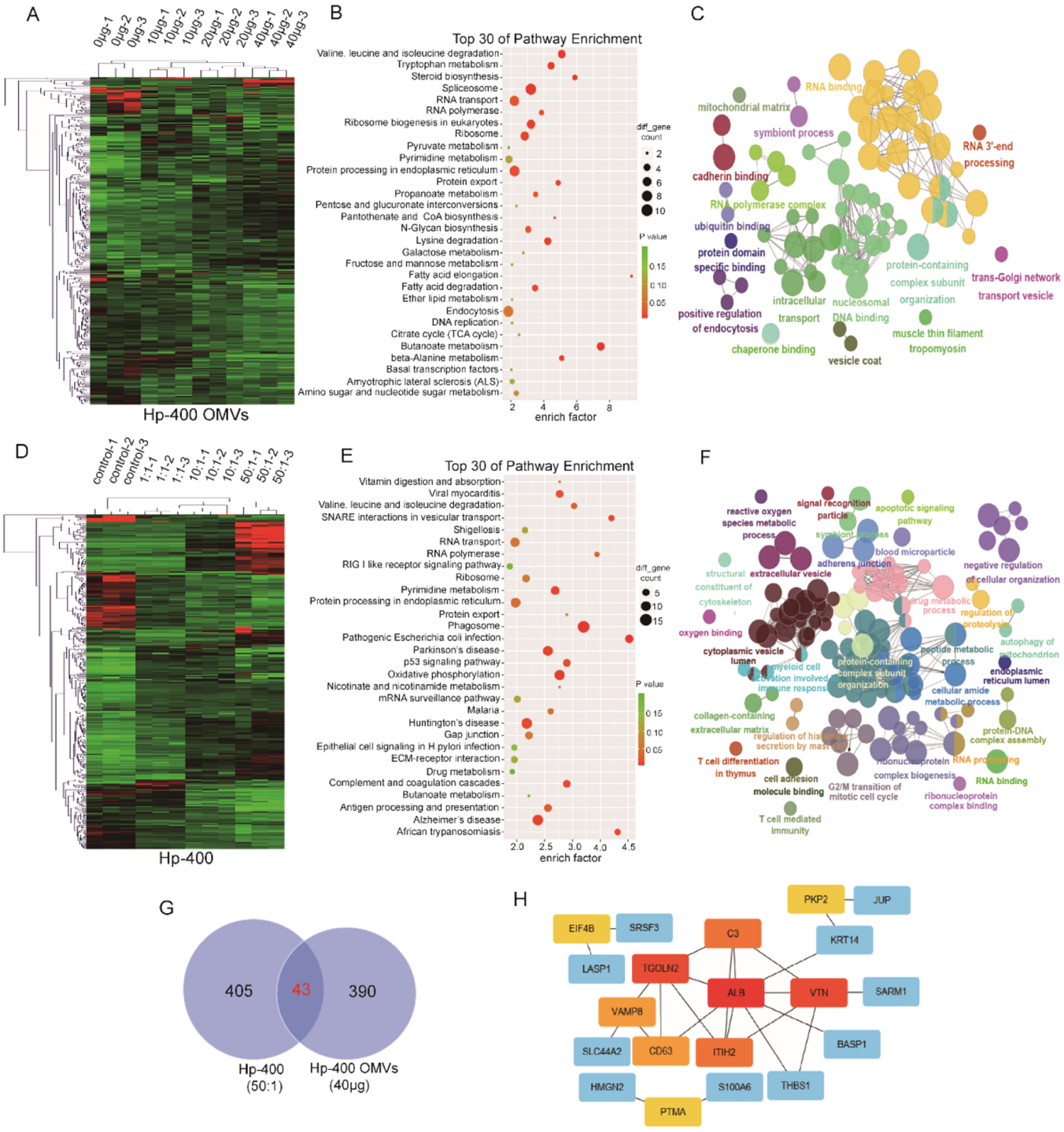

Figure 6. Proteomic changes of GES1 infected by Hp-400 OMVs and bacteria. (A) Heat map showing differentially expressed proteins in different groups of GES1 cocultured with increasing Hp-400 OMVs (0, 10, 20, and 40 μg/well). (B) KEGG analysis of differentially expressed proteins in GES1 control and GES1 cocultured with 40 μg of Hp-400 OMVs. (C) GO analysis of differentially expressed proteins in GES1 control and GES1 cocultured with 40 μg of Hp-400 OMVs. (D) Heat map showing differentially expressed proteins in different groups of GES1 cocultured with increasing Hp-400 (0, 1:1, 10:1, and 50:1). (E) KEGG analysis of differentially expressed proteins in GES1 control and GES1 cocultured with 50:1 Hp-400. (F) GO analysis of differentially expressed proteins in GES1 control and GES1 cocultured with 50:1 Hp-400. (G) Venn diagram revealed the overlapped proteins between differentially expressed proteins in GES1 infected by Hp-400 and OMVs. (H) Top 10 hub genes of the overlapped proteins in panel G.

changes in cadherin binding, endocytosis, mitochondrial matrix, and ubiquitin binding pathways in GES1 cells cultured with 40 μg of OMVs (Figure 6C).

We also detected proteomic changes in GES1 cells cocultured with Hp-400 cells. A total of 4406 proteins were identified, and 243, 307, and 405 proteins were significantly changed (|fold change| > 2) in abundance after infection with Hp-400 at MOIs of 1:1, 10:1, and 50:1, respectively, compared to uninfected samples (Figure 6D and Supporting information Table S4). We characterized changes in the GES1 cell proteome after infection

https://doi.org/10.1021/acsomega.1c04549
ACS Omega 2022, 7, 240−258

A

Gene symbol	Abundance ratio:11637-OMV			Abundance ratio:11637-H.pylori		
	10μg/0μg	20μg/0μg	20μg/0μg	1:1/control	10:1/control	50:1/control
PLG	1.939	1.99	3.098	1.012	1.475	2.424
VTN	2.621	2.573	7.348	1.281	2.057	3.44
F2	4.725	9.657	21.388	1.132	3.271	8.474
THBS1	2.807	4.637	8.308	1.214	1.939	5.227
A2M	11.164	22.79	44.58	1.267	1.554	2.112
C3	3.876	6.288	12.505	0.99	1.734	5.702
ITIH2	10.141	21.519	31.074	1.119	2.252	4.224
F5	3.229	4.586	9.34	1.007	1.632	2.036
LRP1	1.304	1.564	2.682	0.963	0.386	0.336
APOM	2.812	5.99	7.274	1.23	2.281	6.575

B

Gene symbol	Abundance ratio:400-OMV			Abundance ratio:400-H.pylori		
	10μg/0μg	20μg/0μg	20μg/0μg	1:1/control	10:1/control	50:1/control
ALB	0.329	0.453	0.39	0.989	3.177	4.644
VTN	1.326	1.664	2.188	0.885	2.482	4.161
TGOLN2	0.654	0.471	0.507	0.437	0.329	0.474
ITIH2	1.163	3.333	3.596	0.819	3.021	4.467
C3	1.07	1.621	1.941	0.71	4.258	8.266
CD63	0.303	0.4	0.469	0.34	0.381	0.328
VAMP8	0.536	0.521	0.521	0.594	0.671	0.394
PTMA	0.395	0.479	0.392	0.624	0.344	0.349
PKP2	1.12	1.358	1.559	1.556	4.73	25.373
EIF4B	0.75	0.529	0.488	1.855	1.321	2.002

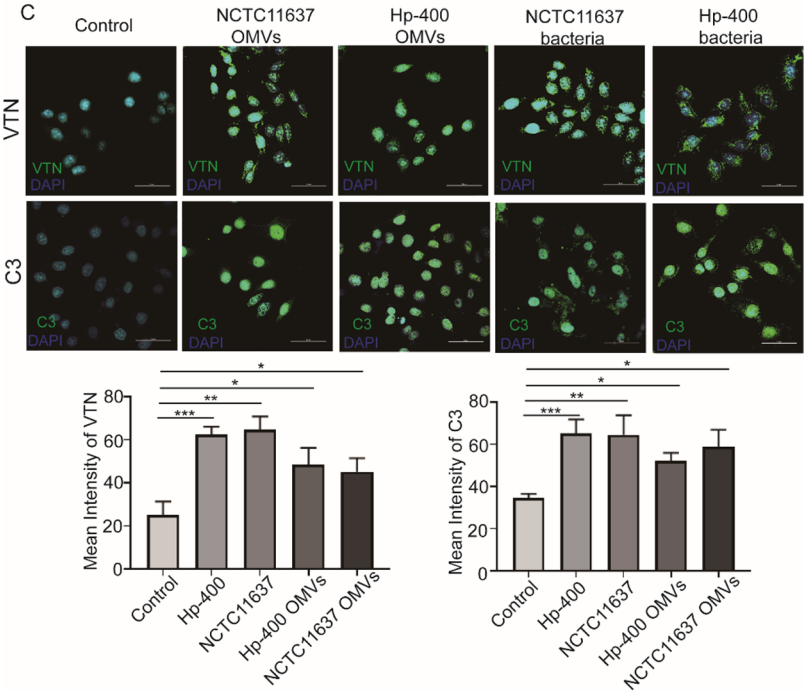

Figure 7. Screening and verification of the hub genes altered both by *H. pylori* and OMVs. (A) Actual expression of hub genes in NCTC11637 and OMV proteomic data. (B) Actual expression of hub genes in Hp-400 and OMV proteomic data. (C) Immunofluorescence analysis of VTN and C3 in GES1 infected by NCTC11637 or Hp-400 or their OMVs. *$p < 0.05$, **$p < 0.01$, ***$p < 0.001$.

with 50:1 Hp-400. The KEGG analysis showed significant changes in oxidative phosphorylation, phagosome, pyrimidine metabolism, and p53 signaling pathways (Figure 6E). In addition, the GO analysis showed that T cell-mediated immunity, apoptosis, protein−DNA complex assembly, and the cell cycle were altered (Figure 6F).

Certain pathways altered by Hp-400 OMVs were also changed in response to Hp-400, including adhesion molecules, RNA polymerase, protein processing in the endoplasmic reticulum, and RNA processing. Forty-three proteins overlapped between Hp-400 OMV- and Hp-400-infected GES1 cells (Figure 6G), of which the top 10 hub genes were screened (Figure 6H). These results further indicated that *H. pylori* affected the proteomes of gastric epithelial cells partially by secreting OMVs.

OMVs and *H. pylori* Mediated the Upregulation of VTN and C3 in GES1 Cells. We integrated the top 10 hub genes shown in Figures 5H and 6H to confirm the common markers of *H. pylori* and OMV infection. Furthermore, we screened the expression abundance of these proteins and found that the levels of most proteins increased progressively with the increase in the concentrations of OMVs or *H. pylori* (Figure 7A,B). Among these proteins, VTN and C3 were both elevated in response to treatments with OMVs and *H. pylori* strains. Hence, we detected the expression of VTN and C3 using laser scanning confocal microscopy (LSCM). Both OMVs and *H. pylori* promoted VTN

https://doi.org/10.1021/acsomega.1c04549
ACS Omega 2022, 7, 240−258

and C3 expressions (Figure 7C). Taken together, we revealed that VTN and C3 were the pathogenic targets of *H. pylori* on gastric epithelium cells by secreting OMVs.

DISCUSSION

In the study, we aimed to demonstrate the pathogenicity of *H. pylori* primarily through secretion of OMVs. OMVs are released by kinds of Gram-negative bacteria and contain proteins, DNA, toxins, peptidoglycan, and lipids, which play roles in the infection process, including helping to build a colonization niche[22] and the delivery of virulence factors and toxins to host cells.[23] We isolated OMVs using size exclusion chromatography (SEC) and identified 436 proteins in NCTC11637 OMVs and 372 proteins in Hp-400 OMVs. The global proteomic analysis of *H. pylori* OMVs illustrated that there were a variety of proteins in OMVs, including well-known toxin proteins of *H. pylori*, which further emphasized the crucial contribution of OMVs to mediate pathogenesis in the host. Several main toxin factors were detected in *H. pylori* OMVs, such as vacA and cagA. The vacA gene is conserved among all *H. pylori* strains, which has the ability to induce cell vacuolation. CagA is a strain-specific *H. pylori* gene that is considered a marker for strains that lead to a high risk of gastric cancer. The delivery of Cag A protein is mainly through the bacterial type four secretion system, which causes a direct effect on epithelial cells, including disrupting cell signaling pathways and cell polarity.[24−26]

H. pylori is reported to have a high degree of genomic diversity because of high frequencies of mutation and recombination.[27−30] Recently, Furuta *et al.* reported multi-locus sequence typing and whole genome sequence analyses of very closely related *H. pylori* strains from the same family members consisting of parents and children in Japan, suggesting adaptation to a new host through mutations in virulence-related genes, restriction-modification genes, and OMP genes.[31,32] In our study, NCTC11637 was the standard strain, and Hp-400 was isolated from gastric tissues from patients in Hebei Province, an area with a high incidence of gastric cancer. These strains induced similar but not identical proteomic changes in GES1 cells, indicating that different strains have different pathogenic mechanisms. The results suggested that precise individualized treatment is necessary in clinical applications.

OMVs serve as vehicles for toxin delivery into host cells to promote bacterial pathogenicity and induce an inflammatory response. In this study, we mimicked the in vivo interaction between *H. pylori* or OMVs and the gastric mucosa through the coculture of GES1 cells and *H. pylori* or OMVs. Inflammatory factors were detected using flow cytometry; we demonstrated that OMVs contribute, at least in part, to driving a robust inflammatory response in gastric epithelial cells. A number of cytokines are elevated when infected by OMVs and *H. pylori*. For example, IL-8 is a potential neutrophil chemoattractant and activating factor that mediates strong pro-inflammatory responses. IL-8 levels are increased by *H. pylori* infection in a cag-dependent manner,[33] and polymorphisms in IL-8 are associated with increased risks of chronic atrophic gastritis and gastric cancer.[34,35] IL-6 is a significant mediator of inflammation that promotes a Th17-mediated inflammatory response. IL-6 expression is associated with the disease status among patients with *H. pylori*-associated gastritis[36] and gastric cancer.[37] TNF-α is a cytokine involved in systemic inflammation and the Th1 response, and TNF levels are increased in patients with *H. pylori*-associated gastritis.[36]

In addition to altering inflammatory signaling pathways, *H. pylori* has also been shown to disrupt cellular junctional complexes[38] and induce cytoskeletal rearrangements that are suggestive of the uncontrolled growth induced by growth factors.[39] *H. pylori* has also been shown to disrupt the balance between gastric epithelial cell proliferation and apoptosis.[40] However, the molecular mechanism of virulence factor delivery via OMVs has been unclear. We speculated that the main function of OMVs is to mimic parental pathogens and induce pathological damage. In addition to the well-established secretion systems, OMVs have been recently considered a new independent secretion system. Many "well-known" virulence factors and toxins have been identified that use OMVs as an alternative secretory pathway. OMVs provide unique advantages compare to other secretion systems by transporting high concentrations of proteins and delivering them to target destinations over long distances. Transmission of bacterial proteins by OMVs into host cells appears to be an important aspect in pathogens. In our study, disease pathways and networks induced by OMVs are directly related to gastrointestinal injury, disease, and development of cancer. These described pathways and networks will allow future functional analyses of specific proteomic targets that have been previously uncharacterized with response to either *H. pylori* infection or gastric carcinogenesis but now may play an important role in the development of gastric injury and cancer. A more thorough understanding of these networks will enable the exploitation of targetable pathways and effectors for clinical benefits and disease prevention.

VTN and complement C3 are two proteins that were detected through label-free mapping and were upregulated upon treatments with *H. pylori* and OMVs from both NCTC11637 and Hp-400. These targets were validated by LSCM, and the data were consistent with the HPLC-MS/MS results. VTN has not been previously identified to be associated with *H. pylori* infection. However, it has been previously shown to promote gastric cancer cell growth and motility in vitro and in vivo. In addition, VTN was also identified as a factor contributing to a poor prognosis of gastric cancer.[41] In contrast, complement C3 has been reported to be activated directly by *H. pylori*,[42] and overexpression of complement C3 correlates with gastric cancer progression by activating the JAK2/STAT3 pathway.[43]

In conclusion, by utilizing proteomic approaches and pathway analyses, we were able to define proteomic changes in GES1 cells in response to *H. pylori* or OMVs infection. These data mirrored alterations observed among humans infected with *H. pylori*, further validating our conjecture that *H. pylori* delivers pathogenic factors by secreting OMVs. Importantly, this technique and approach facilitated the identification and validation of novel protein targets that play important roles in *H. pylori*-induced gastric diseases in individuals at a high risk of infection. Indeed, this technique and approach prospectively accelerates the identification of novel biomarkers that arise in the early inflammatory and carcinogenic cascade and are conductive to therapeutic intervention and disease prevention.

MATERIALS AND METHODS

***H. pylori* Culture.** Two kinds of *H. pylori* were used in the article. The standard strain NCTC11637 was donated by the Shijiazhuang Center for Disease Control and Prevention. The well-characterized clinically isolated *H. pylori* 400 strain was separated from gastric tissues obtained from patients in Hebei Province, which has a high incidence of gastric cancer, and was

https://doi.org/10.1021/acsomega.1c04549
ACS Omega 2022, 7, 240−258

preserved in the China General Microbiological Culture Collection Center (CGMCC 15126). *H. pylori* was cultured for 72 h in a Columbia blood plate medium under microaerobic conditions. *H. pylori* used for OMV isolation was cultured in brain heart infusion broth (BHI, Oxoid) supplemented with 10% fetal bovine serum (BI) and 2% antibiotics for 72 h at 37 °C under microaerobic conditions and with constant rotation (150 rpm).

OMV Preparation and Purification. OMVs were isolated using size exclusion chromatography (SEC).[17] Briefly, after 72 h of incubation, the broth cultures were centrifugated (3000*g*, 15 min) to remove bacteria. The culture supernatants were then filtered via a 0.22 μm filter (Millipore, USA) to eliminate contaminating particles. The filtered supernatant was condensed to 1 mL using Amicon Ultra-15 centrifugal filter units (Millipore, USA) for use in Exosupur columns in accordance with the manufacturer's instructions (Echo Biotech, China). OMVs were collected and condensed to an appropriate volume by centrifugation through Amicon Ultra-4 centrifugal filter units (Millipore, USA). The morphology was characterized using transmission electron microscopy (TEM, JEOL2100F). The particle size distribution and concentration of the OMVs were measured using nanoparticle tracking analysis (NTA).

Cell Culture. The immortalized gastric epithelial cell line, GES1, was obtained from Procell Life Science & Technology (Wuhan, China), which was cultured in RPMI 1640 (Gibco, UA), supplemented with 10% fetal calf serum (BI, Israel), penicillin, and streptomycin (Invitrogen, UA), and incubated at 37 °C with 5% CO_2.

Cytokine Detection. GES1 cells (1×10^5) were seeded in 6-well plates and cultured for 24 h before OMVs and *H. pylori* were added. Forty micrograms of total OMVs or 5×10^6 *H. pylori* were added to each well. After 48 h of coculture, the cellular supernatant was collected for cytokine detection, including IL-2, IL-5, IFN-α, IL-10, IL-6, IFN-γ, IL-8, IL-17, IL-4, IL-12P70, and TNF-α, using flow cytometry in accordance with the manufacturer's instructions (RAISE CARE).

Mass Spectrometry-Based Proteome Profiling. *Protein Extraction and Digestion.* RIPA buffer was added into the *H. pylori* or OMVs cocultured GES1 cells and purified OMVs for protein extraction and then sonicated for 5 s on and 5 s off with a total of six cycles. The proteins were then denatured at 95 °C for 2 min. The insoluble fragment was removed by centrifugation at 12,000*g* for 10 min, and the supernatant was used for the proteomic experiment. The protein concentration was measured using a BCA kit (Thermo).

A filter-aided sample preparation (FASP) procedure was used for protein digestion. Briefly, proteins were loaded in 10 kDa centrifugal filter tubes (Thermo, 88513), the disulfide bond was cleaved with 50 mM DTT in 300 μL UA buffer (8 M urea in 0.1 M Tris−HCl, pH 8.5) for 30 min in 37 °C, alkylated with 50 mM IAA in 300 μL of UA buffer for 30 min in the dark, washed thrice with 300 μL of UA buffer, and then washed twice with 300 μL of 50 mM NH_4HCO_3. All the above steps were centrifuged at 12,000*g* at 25 °C. Proteins were digested at 37 °C for 18 h with trypsin (Promega) at a concentration of 1:100 (w/w) in 50 mM NH_4HCO_3. After digestion, peptides were eluted by centrifugation. Subsequently, peptides were purified and extracted using homemade C18 tips (Empore) in 80% ACN and 2% TFA. Peptides were lyophilized and acidified in 0.1% FA. The peptide concentration was determined by the BCA peptide quantification kit (Thermo).

Proteomic Analysis. For proteomic analysis, the peptides (~1 μg of each sample) were loaded on a nanoflow HPLC Easy-nLC1200 system (Thermo Fisher Scientific), using a 90 min LC gradient at 300 nL/min. Buffer A consisted of 0.1% (v/v) FA in H_2O and buffer B consisted of 0.1% (v/v) FA in 80% ACN. The gradient was set as follows: 2−8% B in 1 min, 8−28% B in 60 min, 28−37% B in 14 min, 37−100% B in 5 min, and 100% B in 10 min. Proteomic analyses were performed on a Q Exactive HF mass spectrometer (Thermo Fisher Scientific). The spray voltage was set at 2100 V in a positive ion mode, and the ion transfer tube temperature was set at 320 °C. Data-dependent acquisition was performed using Xcalibur software in a profile spectrum data type. The MS1 full scan was set at a resolution of 60,000 at m/z 200, AGC target 3e6 and maximum IT 20 ms by an orbitrap mass analyzer (350−1500 m/z), followed by "top 20" MS2 scans generated by higher energy collisional dissociation (HCD) fragmentation at a resolution of 15,000 at m/z 200, AGC target 1e5 and maximum IT 45 ms. The fixed first mass of the MS2 spectrum was set 110.0 m/z. An isolation window was set at 1.6 m/z. The normalized collision energy (NCE) was set at NCE 27%, and the dynamic exclusion time was 45 s. Precursors with charges 1, 8, and >8 were excluded for MS2 analysis.

Database Searching of MS Data. All preliminary data processing was performed in Proteome Discoverer 2.2 using an ion currently-based label-free quantification method or basic protein identification similar to that previously described.[18] Identification of peptides was performed with Sequest HT using a maximum 10 ppm mass tolerance for the parent ion and a 0.02 Da fragment tolerance for tandem mass spectrometry. All data were searched against the UniProtSwissProt Human canonical database (downloaded on Uniprot, 2019) or UniProtSwissProt *H. Pylori* database (downloaded on Uniprot, 2019). Carbamido methylation of cysteines was considered as a static modification; acetylation of the protein N-termini and oxidation of methionine were applied as potential variable modification. Multiple testing corrections were performed using false discovery rate calculations, as previously described.[19] A 1% false discovery rate cutoff was applied to both the peptide spectral matches (calculated using Percolator[20]) and peptide group levels. Quantification ratios for each peptide were determined via pairwise analysis of individual peptides and then averaged for peptide group and protein levels. Significance was then determined by analysis of variance based on the peptide background at both the peptide group and protein levels.[21]

The criterion for differentially expressed proteins was |fold change| > 2. For enrichment analyses, gene ontology (GO) was analyzed using ClueGo of Cytoscape, and the enrichment terms with a p value less than 0.05 was reported. Kyoto Encyclopedia of Genes and Genomes (KEGG) was analyzed online (http://enrich.shbio.com) and the top 30 of enriched pathways were presented in the figures along with the p-value.

Immunofluorescence Assay. GES1 cells were seeded on the glass placed in the 24-well plate in advance, treated with OMVs and *H. pylori* for 24 h. Then, they were fixed with methanol for 6 h at 4 °C and permeabilized by 0.1% Triton X-100. The cells were blocked with sheep serum and incubated with primary antibodies overnight at 4 °C, VTN (A1667, ABclonal) and C3 (A13283, ABclonal). The protein signals were detected by anti-rabbit IgG Fab2 conjugated with Alexa Fluor 488 (Cell Signaling Technology, USA). Finally, the cells

https://doi.org/10.1021/acsomega.1c04549
ACS Omega 2022, 7, 240−258

were incubated with DAPI for 15 min and visualized by a laser confocal microscope (Nikon).

Statistical Analysis. All statistical analyses were performed using SPSS version 13.0 software. All data are presented as the mean ± standard deviation from three independent experiments that were each measured in triplicate. One-way analysis of variance and the student's *t* test were performed for comparison as described. A chi-square test was used to analyze categorical variables. A *p* value of less than 0.05 was considered statistically significant (**p* value < 0.05), and all statistical tests were two-tailed.

■ ASSOCIATED CONTENT

Supporting Information

The Supporting Information is available free of charge at https://pubs.acs.org/doi/10.1021/acsomega.1c04549.

Detailed data of differentially expressed proteins in GES1 cocultured with increasing concentrations of OMVs (0, 10, 20, or 40 μg) and *H. pylori* (1:1, 10:1, or 50:1) in 11,637 and 400 (PDF)

■ AUTHOR INFORMATION

Corresponding Authors

Lianmei Zhao − *Research Center, Hebei Medical University Fourth Affiliated Hospital and Hebei Provincial Tumor Hospital, Shijiazhuang, Hebei Province 050011, China*; Phone: 0311-86095290; Email: lianmeizhmail@163.com

Baoen Shan − *Research Center, Hebei Medical University Fourth Affiliated Hospital and Hebei Provincial Tumor Hospital, Shijiazhuang, Hebei Province 050011, China*; Phone: 0311-86095283; Email: shanbaoen@163.com

Authors

Sisi Wei − *Research Center, Hebei Medical University Fourth Affiliated Hospital and Hebei Provincial Tumor Hospital, Shijiazhuang, Hebei Province 050011, China*; orcid.org/0000-0001-5959-653X

Xiaoya Li − *Research Center, Hebei Medical University Fourth Affiliated Hospital and Hebei Provincial Tumor Hospital, Shijiazhuang, Hebei Province 050011, China*

Jingjing Wang − *Research Center, Hebei Medical University Fourth Affiliated Hospital and Hebei Provincial Tumor Hospital, Shijiazhuang, Hebei Province 050011, China*

Yaojie Wang − *Research Center, Hebei Medical University Fourth Affiliated Hospital and Hebei Provincial Tumor Hospital, Shijiazhuang, Hebei Province 050011, China*

Cong Zhang − *Research Center, Hebei Medical University Fourth Affiliated Hospital and Hebei Provincial Tumor Hospital, Shijiazhuang, Hebei Province 050011, China*

Suli Dai − *Research Center, Hebei Medical University Fourth Affiliated Hospital and Hebei Provincial Tumor Hospital, Shijiazhuang, Hebei Province 050011, China*

Xian Wang − *Shijiazhuang Center for Disease Control and Prevention, Shijiazhuang, Hebei Province 050011, China*

Xiaoqing Deng − *Research Center, Hebei Medical University Fourth Affiliated Hospital and Hebei Provincial Tumor Hospital, Shijiazhuang, Hebei Province 050011, China*

Complete contact information is available at: https://pubs.acs.org/10.1021/acsomega.1c04549

Author Contributions

#S.W. and X.L. contributed equally to this study.

Notes

The authors declare no competing financial interest.

Mass spectrometry experimental data have been deposited on ProteomeXchange Consortium via the PRIDE partner repository with the dataset identifier PXD025216, PXD025259, and PXD025281.

■ ACKNOWLEDGMENTS

This study was supported by the Natural Science Foundation of China (nos. 81772550, 81673642, 81502032, 81973520, and 81902798), the Outstanding Youth Foundation of Hebei Province, China (H2019206697), and the Natural Science Foundation of Hebei Province (H2020206131).

■ ABBREVIATIONS

H. pylori, *Helicobacter pylori*; OMVs, outer membrane vesicles; HPLC-MS/MS, high-performance liquid chromatography−tandem mass spectrometry; GO, gene ontology; KEGG, Kyoto encyclopedia of genes and genomes; MALT, mucosa-associated lymphoid tissue; LPS, lipopolysaccharide; BHI, brain heart infusion; CGMCC, China General Microbiological Culture Collection Center; FBS, fetal bovine serum; SEC, size exclusion chromatography; FASP, filter-aided sample preparation; IAA, indole acetic acid; DTT, dithiothreitol; UA, urea; TFA, trifluoroacetic acid; FA, formic acid; ACN, acetonitrile; NCE, normalized collision energy; PD, proteome discoverer; TEM, transmission electron microscopy; NTA, nanoparticle tracking analysis; C3, complement C3; VTN, vitronectin; LSCM, laser scanning confocal microscope; VEGF, vascular endothelial growth factor

■ REFERENCES

(1) Marshall, B. J.; Warren, J. R. Unidentified curved bacilli in the stomach of patients with gastritis and peptic ulceration. *Lancet* **1984**, *323*, 1311−1315.

(2) Ellis, T. N.; Kuehn, M. J. Virulence and immunomodulatory roles of bacterial outer membrane vesicles. *Microbiol. Mol. Biol. Rev.* **2010**, *74*, 81−94.

(3) Bonnington, K. E.; Kuehn, M. J. Protein selection and export via outer membrane vesicles. *Biochim. Biophys. Acta* **2014**, *1843*, 1612−1619.

(4) Guerrero-Mandujano, A.; Hernández-Cortez, C.; Ibarra, J. A.; Castro-Escarpulli, G. The outer membrane vesicles: Secretion system type zero. *Traffic* **2017**, *18*, 425−432.

(5) Rompikuntal, P. K.; Vdovikova, S.; Duperthuy, M.; Johnson, T. L.; Ahlund, M.; Lundmark, R.; Oscarsson, J.; Sandkvist, M.; Uhlin, B. E.; Wai, S. N. Outer Membrane Vesicle-Mediated Export of Processed PrtV Protease from Vibrio cholerae. *PLoS One* **2015**, *10*, No. e0134098.

(6) Vanaja, S. K.; Russo, A. J.; Behl, B.; Banerjee, I.; Yankova, M.; Deshmukh, S. D.; Rathinam, V. A. K. Bacterial Outer Membrane Vesicles Mediate Cytosolic Localization of LPS and Caspase-11 Activation. *Cell* **2016**, *165*, 1106−1119.

(7) Bielaszewska, M.; Rüter, C.; Bauwens, A.; Greune, L.; Jarosch, K. A.; Steil, D.; Zhang, W.; He, X.; Lloubes, R.; Fruth, A.; Kim, K. S.; Schmidt, M. A.; Dobrindt, U.; Mellmann, A.; Karch, H. Host cell interactions of outer membrane vesicle-associated virulence factors of enterohemorrhagic Escherichia coli O157: Intracellular delivery, trafficking and mechanisms of cell injury. *PLoS Pathog.* **2017**, *13*, No. e1006159.

(8) Kunsmann, L.; Ruter, C.; Bauwens, A.; Greune, L.; Gluder, M.; Kemper, B.; Fruth, A.; Wai, S. N.; He, X.; Lloubes, R.; Schmidt, M. A.; Dobrindt, U.; Mellmann, A.; Karch, H.; Bielaszewska, M. Virulence from vesicles: Novel mechanisms of host cell injury by Escherichia coli O104:H4 outbreak strain. *Sci. Rep.* **2015**, *5*, 13252.

(9) Bomberger, J. M.; Maceachran, D. P.; Coutermarsh, B. A.; Ye, S.; O'Toole, G. A.; Stanton, B. A. Long-distance delivery of bacterial virulence factors by Pseudomonas aeruginosa outer membrane vesicles. *PLoS Pathog.* **2009**, *5*, No. e1000382.
(10) Turner, L.; Bitto, N. J.; Steer, D. L.; Lo, C.; D'Costa, K.; Ramm, G.; Shambrook, M.; Hill, A. F.; Ferrero, R. L.; Kaparakis-Liaskos, M. Helicobacter pylori Outer Membrane Vesicle Size Determines Their Mechanisms of Host Cell Entry and Protein Content. *Front Immunol.* **2018**, *9*, 1466.
(11) Parker, H.; Chitcholtan, K.; Hampton, M. B.; Keenan, J. I. Uptake of Helicobacter pylori outer membrane vesicles by gastric epithelial cells. *Infect. Immun.* **2010**, *78*, 5054−5061.
(12) Kaparakis, M.; Turnbull, L.; Carneiro, L.; Firth, S.; Coleman, H. A.; Parkington, H. C.; Le Bourhis, L.; Karrar, A.; Viala, J.; Mak, J.; Hutton, M. L.; Davies, J. K.; Crack, P. J.; Hertzog, P. J.; Philpott, D. J.; Girardin, S. E.; Whitchurch, C. B.; Ferrero, R. L. Bacterial membrane vesicles deliver peptidoglycan to NOD1 in epithelial cells. *Cell. Microbiol.* **2010**, *12*, 372−385.
(13) Fiocca, R.; Necchi, V.; Sommi, P.; Ricci, V.; Telford, J.; Cover, T. L.; Solcia, E. Release of Helicobacter pylori vacuolating cytotoxin by both a specific secretion pathway and budding of outer membrane vesicles. Uptake of released toxin and vesicles by gastric epithelium. *J. Pathol.* **1999**, *188*, 220−226.
(14) Ismail, S.; Hampton, M. B.; Keenan, J. I. Helicobacter pylori outer membrane vesicles modulate proliferation and interleukin-8 production by gastric epithelial cells. *Infect. Immun.* **2003**, *71*, 5670−5675.
(15) Chitcholtan, K.; Hampton, M. B.; Keenan, J. I. Outer membrane vesicles enhance the carcinogenic potential of Helicobacter pylori. *Carcinogenesis* **2008**, *29*, 2400−2405.
(16) Ko, S. H.; Jeon, J. I.; Kim, Y. J.; Yoon, H. J.; Kim, H.; Kim, N.; Kim, J. S.; Kim, J. M. Helicobacter pylori outer membrane vesicle proteins induce human eosinophil degranulation via a β2 Integrin CD11/CD18- and ICAM-1-dependent mechanism. *Mediators Inflammation* **2015**, *2015*, 301716.
(17) Buschmann, D.; Kirchner, B.; Hermann, S.; Märte, M.; Wurmser, C.; Brandes, F.; Kotschote, S.; Bonin, M.; Steinlein, O. K.; Pfaffl, M. W.; Schelling, G.; Reithmair, M. Evaluation of serum extracellular vesicle isolation methods for profiling miRNAs by next-generation sequencing. *J. Extracell. Vesicles* **2018**, *7*, 1481321.
(18) Shen, X.; Shen, S.; Li, J.; Hu, Q.; Nie, L.; Tu, C.; Wang, X.; Orsburn, B.; Wang, J.; Qu, J. An IonStar Experimental Strategy for MS1 Ion Current-Based Quantification Using Ultrahigh-Field Orbitrap: Reproducible, In-Depth, and Accurate Protein Measurement in Large Cohorts. *J. Proteome Res.* **2017**, *16*, 2445−2456.
(19) The, M.; Tasnim, A.; Kall, L. How to talk about protein-level false discovery rates in shotgun proteomics. *Proteomics* **2016**, *16*, 2461−2469.
(20) Kall, L.; Canterbury, J. D.; Weston, J.; Noble, W. S.; MacCoss, M. J. Semi-supervised learning for peptide identification from shotgun proteomics datasets. *Nat. Methods* **2007**, *4*, 923−925.
(21) Oberg, A. L.; Vitek, O. Statistical design of quantitative mass spectrometry-based proteomic experiments. *J. Proteome Res.* **2009**, *8*, 2144−2156.
(22) Li, Z.; Clarke, A. J.; Beveridge, T. J. Gram-negative bacteria produce membrane vesicles which are capable of killing other bacteria. *J. Bacteriol.* **1998**, *180*, 5478−5483.
(23) Kesty, N. C.; Mason, K. M.; Reedy, M.; Miller, S. E.; Kuehn, M. J. Enterotoxigenic Escherichia coli vesicles target toxin delivery into mammalian cells. *EMBO J* **2004**, *23*, 4538−4549.
(24) Naumann, M. Pathogenicity island-dependent effects of Helicobacter pylori on intracellular signal transduction in epithelial cells. *Int. J. Med. Microbiol.* **2005**, *295*, 335−341.
(25) Bebb, J. R.; Leach, L.; Zaitoun, A.; Hand, N.; Letley, D. P.; Thomas, R.; Atherton, J. C. Effects of Helicobacter pylori on the cadherin-catenin complex. *J. Clin. Pathol.* **2006**, *59*, 1261−1266.
(26) Saadat, I.; Higashi, H.; Obuse, C.; Umeda, M.; Murata-Kamiya, N.; Saito, Y.; Lu, H.; Ohnishi, N.; Azuma, T.; Suzuki, A.; Ohno, S.; Hatakeyama, M. Helicobacter pylori CagA targets PAR1/MARK kinase to disrupt epithelial cell polarity. *Nature* **2007**, *447*, 330−333.
(27) Odenbreit, S.; Haas, R. Helicobacter pylori: impact of gene transfer and the role of the cag pathogenicity island for host adaptation and virulence. *Curr. Top Microbiol. Immunol.* **2002**, *264*, 1−22.
(28) Falush, D.; Kraft, C.; Taylor, N. S.; Correa, P.; Fox, J. G.; Achtman, M.; Suerbaum, S. Recombination and mutation during long-term gastric colonization by Helicobacter pylori: estimates of clock rates, recombination size, and minimal age. *Proc. Natl. Acad. Sci. U. S. A.* **2001**, *98*, 15056−15061.
(29) Yahara, K.; Kawai, M.; Furuta, Y.; Takahashi, N.; Handa, N.; Tsuru, T.; Oshima, K.; Yoshida, M.; Azuma, T.; Hattori, M.; Uchiyama, I.; Kobayashi, I. Genome-wide survey of mutual homologous recombination in a highly sexual bacterial species. *Genome Biol. Evol.* **2012**, *4*, 628−640.
(30) Alm, R. A.; Ling, L. S.; Moir, D. T.; King, B. L.; Brown, E. D.; Doig, P. C.; Smith, D. R.; Noonan, B.; Guild, B. C.; deJonge, B. L.; Carmel, G.; Tummino, P. J.; Caruso, A.; Uria-Nickelsen, M.; Mills, D. M.; Ives, C.; Gibson, R.; Merberg, D.; Mills, S. D.; Jiang, Q.; Taylor, D. E.; Vovis, G. F.; Trust, T. J. Genomic-sequence comparison of two unrelated isolates of the human gastric pathogen Helicobacter pylori. *Nature* **1999**, *397*, 176−180.
(31) Furuta, Y.; Konno, M.; Osaki, T.; Yonezawa, H.; Ishige, T.; Imai, M.; Shiwa, Y.; Shibata-Hatta, M.; Kanesaki, Y.; Yoshikawa, H.; Kamiya, S.; Kobayashi, I. Microevolution of Virulence-Related Genes in Helicobacter pylori Familial Infection. *PLoS One* **2015**, *10*, No. e0127197.
(32) Osaki, T.; Konno, M.; Yonezawa, H.; Hojo, F.; Zaman, C.; Takahashi, M.; Fujiwara, S.; Kamiya, S. Analysis of intra-familial transmission of Helicobacter pylori in Japanese families. *J. Med. Microbiol.* **2015**, *64*, 67−73.
(33) Crabtree, J. E.; Farmery, S. M.; Lindley, I. J.; Figura, N.; Peichl, P.; Tompkins, D. S. CagA/cytotoxic strains of Helicobacter pylori and interleukin-8 in gastric epithelial cell lines. *J.;Clin. Pathol.* **1994**, *47*, 945−950.
(34) de Oliveira, J. G.; Rossi, A. F.; Nizato, D. M.; Cadamuro, A. C.; Jorge, Y. C.; Valsechi, M. C.; Venancio, L. P.; Rahal, P.; Pavarino, E. C.; Goloni-Bertollo, E. M.; Silva, A. E. Influence of functional polymorphisms in TNF-alpha, IL-8, and IL-10 cytokine genes on mRNA expression levels and risk of gastric cancer. *Tumour Biol.* **2015**, *36*, 9159−9170.
(35) Wang, Y. M.; Li, Z. X.; Tang, F. B.; Zhang, Y.; Zhou, T.; Zhang, L.; Ma, J. L.; You, W. C.; Pan, K. F. Association of genetic polymorphisms of interleukins with gastric cancer and precancerous gastric lesions in a high-risk Chinese population. *Tumour Biol.* **2016**, *37*, 2233−2242.
(36) Crabtree, J. E.; Shallcross, T. M.; Heatley, R. V.; Wyatt, J. I. Mucosal tumour necrosis factor alpha and interleukin-6 in patients with Helicobacter pylori associated gastritis. *Gut* **1991**, *32*, 1473−1477.
(37) Wu, C. W.; Wang, S. R.; Chao, M. F.; Wu, T. C.; Lui, W. Y.; P'Eng F, K.; Chi, C. W. Serum interleukin-6 levels reflect disease status of gastric cancer. *Am. J. Gastroenterol.* **1996**, *91*, 1417−1422.
(38) Backert, S.; Schmidt, T. P.; Harrer, A.; Wessler, S. Exploiting the Gastric Epithelial Barrier: Helicobacter pylori's Attack on Tight and Adherens Junctions. *Curr. Top Microbiol. Immunol.* **2017**, *400*, 195−226.
(39) Tegtmeyer, N.; Neddermann, M.; Asche, C. I.; Backert, S. Subversion of host kinases: a key network in cellular signaling hijacked by Helicobacter pylori CagA. *Mol. Microbiol.* **2017**, *105*, 358−372.
(40) Meng, W.; Bai, B.; Sheng, L.; Li, Y.; Yue, P.; Li, X.; Qiao, L. Role of Helicobacter pylori in gastric cancer: advances and controversies. *Discov. Med.* **2015**, *20*, 285−293.
(41) Lian, L.; Li, X. L.; Xu, M. D.; Li, X. M.; Wu, M. Y.; Zhang, Y.; Tao, M.; Li, W.; Shen, X. M.; Zhou, C.; Jiang, M. VEGFR2 promotes tumorigenesis and metastasis in a pro-angiogenic-independent way in gastric cancer. *BMC Cancer* **2019**, *19*, 183.
(42) Berstad, A. E.; Hogasen, K.; Bukholm, G.; Moran, A. P.; Brandtzaeg, P. Complement activation directly induced by Helicobacter pylori. *Gastroenterology* **2001**, *120*, 1108−1116.

https://doi.org/10.1021/acsomega.1c04549
ACS Omega 2022, 7, 240−258

(43) Yuan, K.; Ye, J.; Liu, Z.; Ren, Y.; He, W.; Xu, J.; He, Y.; Yuan, Y. Complement C3 overexpression activates JAK2/STAT3 pathway and correlates with gastric cancer progression. *J. Exp. Clin. Cancer Res.* **2020**, *39*, 9.

https://doi.org/10.1021/acsomega.1c04549
ACS Omega 2022, 7, 240−258